Respiratory Syncytial Virus M2-1 Protein Requires Phosphorylation for Efficient Function and Binds Viral RNA during Infection

TARA L. CARTEE AND GAIL W. WERTZ*

Department of Microbiology, University of Alabama School of Medicine, Birmingham, Alabama 35294

The M2-1 protein of respiratory syncytial (RS) virus is a transcriptional processivity and antitermination factor. The M2-1 protein has a Cys3His1 zinc binding motif which is essential for function, is phosphorylated, and has been shown to interact with the RS virus nucleocapsid (N) protein. In the work reported here, we determined the sites at which the M2-1 protein was phosphorylated and investigated the importance of these phosphorylated residues for M2-1 function in transcription. By combining protease digestion, matrix-assisted laser desorption ionization–time of flight mass spectrometry, and site-directed mutagenesis, we identified the phosphorylated residues as serines 58 and 61, not threonine 56 and serine 58 as previously reported. Serines 58 and 61 and the surrounding amino acids are in a consensus sequence for phosphorylation by casein kinase I. Consistent with this, we showed that the unphosphorylated M2-1 protein synthesized in *Escherichia coli* could be phosphorylated in vitro by casein kinase I. The effect of eliminating phosphorylation by site-specific mutagenesis of serines 58 and 61 on the function of the M2-1 protein in transcription of RS virus subgenomic replicons was assayed. The activities of the M2-1 protein phosphorylation mutants in transcriptional antitermination were tested over a range of concentrations and were found to be substantially inhibited at all concentrations. The data show that phosphorylation is important for the M2-1 protein function in transcription. However, mutation of the M2-1 phosphorylation sites did not interfere with the ability of the M2-1 protein to interact with the N protein in transfected cells. The interaction of the M2-1 and N proteins in cotransfected cells was found to be sensitive to RNase A, indicating that the M2-1–N protein interaction was mediated via RNA. Furthermore, the M2-1 protein was shown to bind monocistronic and polycistronic RS virus mRNAs during infection.

Respiratory syncytial (RS) virus is an important human pathogen that causes lower respiratory tract infection in children. RS virus is a member of the genus *Pneumovirus* in the family *Paramyxoviridae*. Members of this family are nonsegmented, negative-sense, single-stranded RNA viruses. The RS virus genome contains 10 genes, encoding at least 11 proteins (6, 7). Three of the RS virus gene products are essential for RNA replication: the nucleocapsid (N) protein, which encapsidates the viral genome, and the large polymerase protein (L) and the phosphoprotein (P), which comprise the viral RNA-dependent RNA polymerase (RdRp) (13, 32, 36).

In contrast to replication, efficient transcription of RS mRNAs requires an additional gene product, the M2-1 protein. The M2-1 protein is encoded by the first of two open reading frames (ORFs) of the M2 gene (5, 8). The second ORF of the M2 gene encodes the M2-2 protein. The M2-1 protein is a basic phosphoprotein of 194 amino acids that functions in transcription as a processivity factor and an antiterminator (4, 16). M2-1 colocalizes with the N protein in cytoplasmic inclusions and interacts with the N protein, as assayed by coimmunoprecipitation with a monoclonal antibody (MAb) to M2-1 (12, 15). There is a conserved Cys3His1 motif, predicted to bind zinc, at the amino terminus of the M2-1 protein, and maintenance of the predicted zinc coordinating

residues is essential for the function of the protein (15). Mutation of the cysteine or histidine residues of this motif results in a loss of M2-1 phosphorylation, loss of the M2-1–N interaction, and loss of M2-1 transcriptional activity (15). Although, it has not been directly demonstrated that this motif in M2-1 binds zinc, it is apparent that maintenance of the motif is required for activity. The M2-1 protein in RS virus-infected cells exists in different phosphorylation states, resulting in its migration as at least two bands by reducing sodium dodecyl sulfate-polyacrylamide gel electrophoresis (SDS-PAGE) (15, 23, 30); the slower-migrating species contains the majority of the phosphorylated form, and the faster-migrating species lacks significant phosphorylation. The sites of M2-1 phosphorylation were recently reported as threonine 56 and serine 58 (9). The contribution of phosphorylation to the function of M2-1 has not been investigated.

As with other negative-strand viruses, transcription of RS viral genes is obligatorily sequential. The RdRp enters at or near the 3′ end of the genome, and genes are transcribed in order from the 3′ to the 5′ end of the genome (10). Attenuation occurs at each gene junction, resulting in a gradient of mRNA synthesis such that genes nearest the 3′ end of the genome are transcribed more abundantly than those near the 5′ end (2, 10). The junctions between RS virus genes contain semiconserved gene end and conserved gene start sequences separated by nonconserved intergenic sequences of various lengths (3). The gene end sequence contains the signals for the RS virus RdRp to polyadenylate and terminate synthesis of the mRNA (3, 19, 21). However, the efficiency of termination at

* Corresponding author. Mailing address: Department of Microbiology, University of Alabama School of Medicine, BBRB Box 17, Room 366, 845 19th St. South, Birmingham, AL 35294. Phone: (205) 934-0877. Fax: (205) 934-1636. E-mail: gail_wertz@microbio.uab.edu.

the various RS virus gene junctions differs (14). The conserved gene start sequence signals initiation of a new mRNA (20). In order to initiate synthesis of the new mRNA, the RdRp must first terminate synthesis of the upstream message (17, 21).

The M2-1 protein functions as both a transcriptional processivity factor and an antiterminator (4, 16). The M2-1 processivity function prevents intragenic termination, allowing the synthesis of full-length mRNAs (11), and the antitermination function causes the RdRp to ignore the semiconserved gene end sequence (14, 16), resulting in the synthesis of polycistronic RNAs observed in infection. The relative contributions of processivity and antitermination to the function of M2-1 have not been clearly discriminated. Both of these features of M2-1 may be necessary to allow deeper access of the RS virus RdRp on the genomic template, which is potentially important, given that pneumovirus genomes are longer and contain more genes than those of most paramyxovirus members. In addition, the various RS virus genes respond differently to the M2-1 protein (11, 14). This differential sensitivity may represent a mechanism by which the virus further regulates the expression of certain gene products.

In the work reported here, we first determined the number and location of phosphorylated residues in the M2-1 protein, and our results show that serines 58 and 61 are phosphorylated, in contrast to a previous report (9). We next examined the effect of eliminating phosphorylation, by site-specific mutagenesis of individual sites or sites in combination, on the function of the M2-1 protein as a transcriptional antiterminator and on its interaction with the N protein. Our data show that phosphorylation is important for the M2-1 protein function in transcription. Further, we show that the M2-1 protein binds viral mRNAs in infected cells and that the interaction of the M2-1 and N proteins in transfected cells is mediated by RNA.

MATERIALS AND METHODS

cDNA constructs. The RS virus-specific plasmids pN, pP, pL, pM2ORF1, pC7S, pF/M2, and pM/SH have been previously described (14–16, 36).

A cDNA designed to express a carboxy-terminal six-histidine-tagged M2-1 protein (pM2-6His) was generated by PCR of pM2ORF1 using a set of three nested primers to add nucleotides encoding a thrombin cleavage site and a six-His tag to the 5′ end of the genomic M2-1 coding sequence. The *Kpn*I- and *Bam*HI-digested PCR product was cloned into the respective sites in pGEM3 (Promega) oriented for expression by the T7 promoter. This construct contains the following 12 amino acids attached to the carboxy terminus of M2-1: LVPRG SHHHHHH. This construct was tested for its transcriptional activity, phosphorylation state, and ability to interact with the N protein and was found to have wild-type (wt) activity in all respects.

cDNAs expressing mutant M2-1 proteins (pS58A, pS61A, pT56A, and pT56AS58A) were generated in a wt pM2ORF1 background using Quikchange (Stratagene) with complementary mutagenic primers.

A cDNA encoding a glutathione *S*-transferase (GST)-tagged M2-1 protein (GST-M2) was generated for expression in *Escherichia coli*. An M2-1 PCR product from pM2ORF1 was cloned into the *Eco*RI- and *Bam*HI-digested pGEX-1λT (Pharmacia-Biotech). This was designed to produce a fusion protein that contained GST at the amino terminus and the M2-1 protein at the carboxy terminus, with a thrombin cleavage site between them. Thrombin cleavage of the fusion protein resulted in the addition of two amino acids, a glycine and a serine, to the amino terminus of the M2-1 protein.

Nucleotide sequencing of all of the engineered cDNA constructs was performed by the University of Alabama at Birmingham (UAB) Automated DNA Sequence Core Facility on a Perkin-Elmer Applied Biosystems 377 sequencer.

Cells, virus, and cDNA transfections. HEp-2 cells were grown in minimal essential medium (Gibco) supplemented with 5% fetal calf serum. Human RS virus strain A2 or cDNA clones derived from human RS virus strain A2 were used in all experiments. RS virus infections of HEp-2 cells were carried out at a multiplicity of infection (MOI) of 10. Virus was allowed to adsorb for 1.5 h, and then minimal essential medium with 2% fetal calf serum was added. Plasmids encoding RS virus proteins or subgenomic replicons were transfected with Lipofectin into HEp-2 cells previously infected with vTF7-3 or MVA-T7 as described previously (14, 15).

M2-6His expression and MALDI-TOF analysis. The M2-1 protein with a six-His tag (M2-6His) was expressed from vTF7-3-infected (MOI = 5) HEp-2 cells transfected with 14 μg of pM2-6His in 100-mm-diameter dishes. Cells were harvested 18 h posttransfection (p.t.) by freeze-thaw in native binding buffer (20 mM sodium phosphate, 500 mM sodium chloride, 10 mM imidazole, pH 7.8). The clarified lysate from one 100-mm-diameter dish was incubated with 30 μl of nickel-nitriloacetic acid (NiNTA) beads (Qiagen) for 30 min and then washed three times with native wash buffer (20 mM sodium phosphate, 500 mM sodium chloride, 20 mM imidazole, pH 6.0). The NiNTA beads were boiled in denaturing sample buffer, and the partially purified protein was separated by electrophoresis on an SDS–11% polyacrylamide gel. The bands corresponding to the M2-6His protein were excised from the gel, and the gel slice containing M2-6His was destained (25 mM ammonium bicarbonate, 50% acetonitrile), dried, and then cleaved with trypsin, Lys C, or cyanogen bromide (CNBr; Roche). The trypsin used in these experiments contained chymotrypsin activity, as it consistently cleaved M2-1 at amino acid 83. Trypsin and Lys C digestions were performed in 25 mM ammonium bicarbonate. Peptides were extracted three times (50% acetonitrile, 10% formic acid), dried, dissolved in extraction buffer, and diluted 1:10 in αcyano-4-hydroxycinnamic acid (Sigma). CNBr cleavage of M2-1 protein and extraction of peptides were performed in 50% formic acid followed by dilution in sinapinac acid (Sigma). The resultant peptides from the digestions were analyzed by matrix-assisted laser desorption ionization–time of flight mass spectrometry (MALDI-TOF MS) performed by the UAB Comprehensive Cancer Center Mass Spectrometry Shared Facility on a Voyager Elite MALDI-TOF spectrometer (PerSeptive Biosystems) in linear mode. A portion of the cleaved sample was treated with 1 U of calf intestinal phosphatase (CIP; Pharmacia Biotech) for 30 min at 37°C and analyzed. Uncleaved protein was prepared and extracted as for trypsin and Lys C digestions, except the protein was diluted in sinapinac acid as the matrix.

The phosphorylated 53-to-83 peptide was recovered from the protease digestion using an immobilized metal affinity chromatography tip (NEST Group). The negative charge of the phosphates allowed binding to the positively charged column. The column was stripped (50 mM EDTA, 1 M NaCl) and charged with 100 mM ferric chloride in 0.1 M acetic acid. The peptides were eluted with 0.1% ammonium acetate (pH 9.5). The eluted peptide was digested with carboxypeptidase Y using the Sequazyme C-Peptide Sequencing Kit (PerSeptive Biosystems) according to the manufacturer's instructions. The resultant fragments were analyzed by MALDI-TOF MS as described above to confirm the identity of the fragment.

Protein labeling and immunoprecipitation. Expression of the wt or mutant M2-1 protein without histidine tags was assayed by transfecting 5 μg of the appropriate plasmid, using Lipofectin, into vTF7-3-infected HEp-2 cells in 60-mm-diameter dishes. Analysis of N protein interaction with M2-1 protein was performed by transfecting 5 μg of pN alone or with 5 μg of M2-1-encoding plasmid into vTF7-3-infected HEp-2 cells. RS virus-infected or transfected cells, following incubation at 37°C for 20 or 17 h, respectively, were treated with either cysteine- and methionine-deficient or phosphate-deficient medium for 30 min. The infected or transfected cells were labeled for 3 h using 66 μCi of [^{35}S]methionine and [^{35}S]cysteine (Trans ^{35}S label; ICN) per ml or 100 μCi of inorganic [^{33}P]phosphate (ICN) per ml. Cytoplasmic extracts were prepared as described previously (28).

Immunoprecipitations were performed using an anti-M2-1 monoclonal antibody (MAb), ICI3, and protein G-Sepharose (Pharmacia-Biotech). To reduce nonspecific background, the lysates were precleared with a vaccinia virus polyclonal antibody (indicated in the figure legends). RNase A (Sigma), proteinase K (Sigma), DNase RQI (Promega), and protein phosphatase lambda (λ-PPase; New England Biolabs) treatments were performed on the immunoprecipitated protein (indicated in the figure legends). Treatment of the M2-1–N interaction with these reagents was followed by two washes with wash buffer (150 mM NaCl, 10 mM Tris HCl, 1% NP-40, 0.5% deoxycholate, 0.1% SDS). The immunoprecipitated proteins were analyzed by electrophoresis on an SDS–11% polyacrylamide gel and detected by autoradiography. The percent M2-1–N interaction was determined by densitometric analysis of an autoradiogram. The background of the N-only lane was subtracted from each of the cotransfected lanes. Then, a ratio of N to M2-1 was calculated for each lane and compared to the wt M2-1–N interaction by dividing each by the wt ratio, which set the wt interaction to 100%.

GST-M2 protein purification and in vitro phosphorylation. pGST-M2 encoding the cDNA for expression of the GST-M2 fusion protein was transformed into BL21-DE3 cells. Cultures were grown in Luria broth to an optical density of 0.6 and then induced with isopropyl β-D-thiogalactoside at a final concentration of 0.1 mM for 2 h. The cells were lysed by sonication in phosphate-buffered saline (PBS; 140 mM NaCl, 2.7 mM KCl, 10 mM Na_2HPO_4, 1.8 mM KH_2PO_4, pH 7.3). The extract was incubated with glutathione-Sepharose 4B beads (Pharmacia-Biotech) and washed with PBS in the presence of 20 μg of phenylmethylsulfonyl fluoride/ml, and M2-1 was freed from the column by thrombin cleavage (50 U/ml; Pharmacia Biotech) in PBS for 2 h. The eluted protein was analyzed for purity by SDS-PAGE followed by staining with GelCode Blue (Pierce).

The ability of the M2-1 protein to be phosphorylated by casein kinase I (CKI; New England Biolabs) was assayed by incubation in the presence of CKI (60 U) and $[\gamma\text{-}^{33}P]ATP$ (0.6 μCi; NEN) followed by electrophoresis on an SDS–11% polyacrylamide gel, staining with GelCode Blue, and autoradiography.

RNA synthesis. RNA synthesis was analyzed in either RS virus-infected HEp-2 cells or MVA-T7-infected HEp-2 cells transfected with plasmids expressing subgenomic replicons. HEp-2 cells infected with RS virus in 100-mm-diameter dishes were incubated at 37°C for 20 h. Before being labeled, infected cells were pretreated with actinomycin D (Act D; 10 μg/ml; Sigma) for 30 min. RS virus-infected cells were labeled for 5.5 h with 100 μCi of inorganic $[^{33}P]$phosphate per ml in the presence of Act D. Transfections with subgenomic replicons were performed as previously described (14), except that the following amounts of plasmids were used: 4 μg of pF/M2 or pM/SH, 1.5 μg of pN, 0.75 μg of pP, 0.25 μg of pL, and various amounts of M2-1-encoding plasmid. Cytoplasmic extracts were prepared from the infected and transfected cells (28), and RNAs were phenol extracted, ethanol precipitated, separated on a 1.75% agarose–6 M urea gel (34), and detected by fluorography as previously described (24). Quantitation of the RNAs was performed as previously described (14).

Viral RNA coimmunoprecipitations were performed as described in "Protein labeling and immunoprecipitation" above, with MAbs to M2-1 (ICI3; a gift of G. Toms) and N and F proteins (MAb 15 and MAb 19; gifts of G. Taylor). The inorganic $[^{33}P]$phosphate-labeled RNAs were released from the coimmunoprecipitation reaction mixture by boiling it in NTE (100 mM NaCl, 1 mM EDTA, 10 mM Tris) with 0.5% SDS. RNAs were analyzed by phenol extraction, ethanol precipitation, and separation on agarose-urea gels.

RESULTS

Mapping of phosphorylated residues. Initially, mutagenesis was performed to determine the site(s) of phosphorylation of the M2-1 protein. Several sites were chosen for mutagenesis based on similarity with consensus protein kinase C (PKC) and CKII phosphorylation motifs. The potential residues (serines 2 and 108 and threonines 69, 181, 193, and 194) were individually changed to alanine. None of these mutants displayed any change in phosphorylation state (R. Hardy, unpublished data). Since the mutagenesis of potential consensus sites had not revealed the phosphorylation sites, we sought instead to map regions of the M2-1 protein that were phosphorylated by combining protease digestion with MALDI-TOF MS analysis. This technique allows the detection of posttranslational modifications, such as phosphorylation, based on an increase in the mass of the modified fragment (25). Each single phosphorylation event should result in an 80-Da increase in the mass of a peptide. A six-histidine-tagged M2-1 protein, M2-6His, was expressed in HEp-2 cells from pM2-6His, partially purified, and separated by SDS-PAGE, and bands corresponding to the M2-6His protein were excised; cleaved with trypsin, Lys C, or CNBr; and analyzed by MALDI-TOF. The CNBr cleavages were performed on only the slower-migrating species of M2-6His (the phosphorylated form), whereas the protease digestions were performed on a gel slice containing both species of the protein. The cleavage reactions were analyzed for fragments with the expected mass for unphosphorylated and phosphorylated fragments. CNBr cleavage of the phosphorylated (slower-migrating) form of M2-6His resulted in fragments cor-
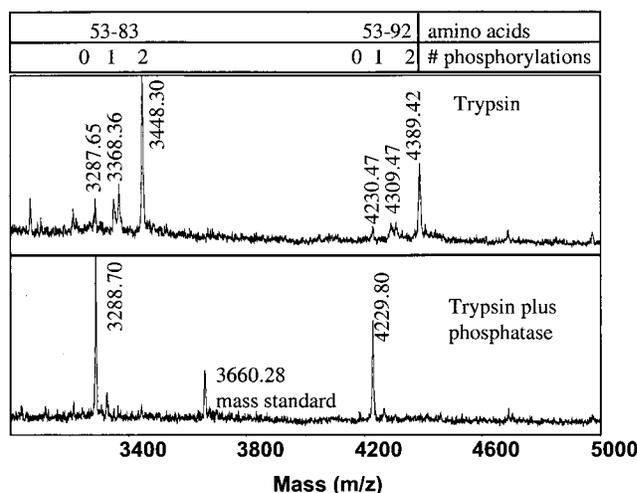
FIG. 1. MALDI-TOF analysis of M2-6His digestion products. (A) Representative trypsin digestion of M2-6His, identifying phosphorylated peptides. M2-6His was transfected into vTF7-3-infected HEp-2 cells. After partial purification with NiNTA beads, the M2-1 protein was separated by electrophoresis on an SDS–11% polyacrylamide gel, stained, excised from the gel, destained, dried, and cleaved with trypsin. The resultant peptides were analyzed by MALDI-TOF in linear mode (top). A duplicate sample was treated with CIP (1 U) for 30 min at 30°C and analyzed (bottom). In the bottom graph, a mass calibration standard (mass standard) was added to the reaction prior to analysis. (B) Potential phosphorylation sites between amino acids 53 and 68 of the M2-1 protein. Mutagenesis was performed on the residues that are underlined and in boldface.

responding to amino acids 100 to 206 and 51 to 206. The 100-to-206 fragment was the expected mass for the unphosphorylated fragment, which indicated that the carboxy-terminal half of the M2-1 protein was not phosphorylated. The fragment corresponding to amino acids 51 to 206 was observed as the expected mass plus approximately 160 Da, indicating that the M2-1 protein was phosphorylated at two locations between amino acids 51 and 100 (data not shown).

Trypsin and Lys C digestions were performed on M2-6His to further narrow the location of the phosphorylation sites. Representative data for M2-6His cleaved with trypsin are shown in Fig. 1A. Two sets of fragments were observed, one peptide corresponding to amino acids 53 to 83 and one peptide corresponding to amino acids 53 to 92, each of which was phosphorylated zero, one, or two times (Fig. 1A, top, and Table 1). Treatment with CIP prior to analysis by MALDI-TOF resulted in the disappearance of the fragments increased in mass by 80 and 160 Da, confirming that the increased mass was due to phosphorylation of the 53-to-83 and 53-to-92 peptides (Fig. 1A, bottom). A summary of the phosphorylated fragments, observed with Lys C or trypsin cleavage, is shown in Table 1. All of the phosphorylated fragments shown in Table 1 were

TABLE 1. Characteristics of phosphorylated fragments observed with Lys C or trypsin cleavage

Protease	Peptide	Observed mass[a]	Mass difference[b]	Inferred no. of phosphorylations	Sensitivity to phosphatase treatment[c]
Trypsin	53–83	3,287.65 (0.08)	0	0	−
		3,368.36 (0.79)	80.71	1	+
		3,448.30 (0.73)	160.65	2	+
	53–92	4,230.47 (0.77)	0	0	−
		4,309.47 (0.21)	79.0	1	+
		4,389.42 (0.24)	158.95	2	+
Lys C	53–80	2,910.23 (1.01)	0	0	−
		2,990.06 (0.84)	79.83	1	+
		3,070.06 (0.84)	159.83	2	+
	53–92	4,230.84 (1.14)	0	0	−
		4,311.95 (2.27)	81.11	1	+
		4,391.35 (1.69)	160.51	2	+

[a] Numbers in parentheses represent the differences between the expected and observed masses. Masses are in daltons.

[b] Mass differences equal to the observed mass of the phosphorylated peptide minus the observed mass of the unphosphorylated peptide. Masses are in daltons.

[c] +, peak disappeared upon phosphatase treatment; −, no change in mass upon phosphatase treatment.

sensitive to phosphatase treatment. No phosphorylated fragments were observed elsewhere in the M2-1 protein. Amino acids 1 to 28 of M2-6His were not observed among any of the proteolytic fragments from any of the digests, making it difficult to rule out the possibility that M2-1 was not phosphorylated in that region, but subsequent mutagenesis showed that the phosphorylation sites resided elsewhere.

The identity of the peptide containing residues 53 to 83 was confirmed by isolation of the phosphorylated peptide on an immobilized metal affinity column followed by carboxypeptidase cleavage and MALDI-TOF analysis. Carboxypeptidase cleavage resulted in a series of fragments corresponding to amino acids 53 to 68, 71, 72, 73, 76, 77, 78, or 82. Each of these fragments was the expected mass plus approximately 160 Da, indicating that the two phosphorylated residues were not located C terminally of the arginine at position 68 (data not shown), narrowing the two phosphorylation sites to amino acids 53 to 68.

Identification of phosphorylation sites. To further investigate the sites of phosphorylation in the M2-1 protein, site-directed mutagenesis was performed on residues that could act as potential phosphate acceptors between amino acids 53 and 68, as shown in Fig. 1B. Serines 58 and 61 which were in a consensus sequence for phosphorylation by CKI, and threonine 56, which was in a consensus sequence for phosphorylation by CKII, were individually changed to alanine (S58A, S61A, and T56A) by site-specific mutagenesis of pM2-ORF1. In addition, a double mutant was made in which threonine 56 and serine 58 were both changed to alanine (T56A S58A). These plasmids were individually transfected into vTF7-3-infected HEp-2 cells. The cells from duplicate transfections were labeled with [35S]methionine and [35S]cysteine or with inorganic [33P]phosphate. The labeled proteins were immunoprecipitated with an anti-M2-1 MAb, ICI3, which has been shown to recognize the different phosphoforms of M2-1 (15). Analysis by SDS-PAGE showed that wt M2-1 migrated as two bands, differentiated by their phosphorylation states (15). The slower-migrating form was predominant, and labeling with 33P indi-

cated that this form was phosphorylated (Fig. 2A, lanes 3 and 4). Treatment of wt M2-1 with λ-PPase resulted in a change in mobility to the faster-migrating form and loss of 33P incorporation (Fig. 2A, lanes 13 and 14), confirming that the observed change in mobility and inorganic [33P]phosphate incorporation were due to phosphorylation. In contrast to wt M2-1, the S58A mutant migrated predominantly as the faster form with a loss of the majority of the 33P incorporation, indicating a lack of phosphorylation (Fig. 2A, lanes 7 and 8). The S61A mutant resulted in a change in the distribution of the two bands, which correlated with a decrease in the phosphorylated form (Fig. 2A, lanes 5 and 6). The double mutant, T56A S58A, had the same phenotype as the S58A single mutant (Fig. 2A, lanes 9 and 10). The T56A mutant was wt in its phosphorylation pattern (Fig. 2A, lanes 11 and 12), which indicated that threonine 56 was not one of the phosphorylated residues. A large amount of a 33P-labeled material coimmunoprecipitated with M2-1 and the mutant M2-1 proteins, as indicated by the labeled material migrating at the top of each 33P-labeled lane (Fig. 2A). The identification of this material is discussed below.

As mentioned previously, analysis of the amino acid sequence surrounding the phosphorylated residues indicated that serine 58 was a potential site for phosphorylation by CKI. The consensus sequence for CKI phosphorylation is an acidic residue followed by any two or three amino acids and then the phosphorylatable serine or threonine. The acidic residue can be an aspartic acid, glutamic acid, phosphoserine, or phosphothreonine (29). Phosphorylation at serine 58 provided a phosphoserine at that position and created a potential CKI phosphoacceptor site at serine 61. Thus, CKI phosphorylation at serine 61 is predicted to be dependent upon prior phosphorylation of serine 58, explaining the lack of phosphorylation of the S58A single mutant.

To test whether CKI could phosphorylate the M2-1 protein, an unphosphorylated M2-1 was produced in *E. coli* as a GST-M2 fusion. Thrombin cleavage of GST-M2, while it was bound on the column, allowed elution of M2-1 and retention of GST. Incubation of the purified M2-1 with CKI and [γ-33P]ATP resulted in a change in migration to a slower-migrating species, which incorporated 33P (Fig. 2C). Additionally, MALDI-TOF analysis of the bacterially expressed M2-1 protein after incubation with CKI indicated that the increase in mass was consistent with two phosphorylation events. Trypsin cleavage followed by MALDI-TOF analysis located the phosphorylation sites in the bacterially expressed M2-1, which had been incubated with CKI, to amino acids 53 to 92, which overlapped with the CKI sites predicted by sequence analysis (data not shown). Neither CKII nor PKC, which were also tested, phosphorylated M2-1 (Hardy, unpublished).

Effect of phosphorylation mutants on antitermination. The M2-1 protein has been characterized as a transcription factor that increases processivity and decreases termination within genes and at the semiconserved gene end termination sequences, resulting in increased production of full-length monocistronic and dicistronic mRNAs (14, 16). The significance of phosphorylation of the M2-1 protein in transcription has not been investigated. The effect of phosphorylation on M2-1 function as an antiterminator was assayed using a dicistronic subgenomic replicon, pF/M2, which contained the F/M2 gene junction in its authentic upstream and downstream sequence
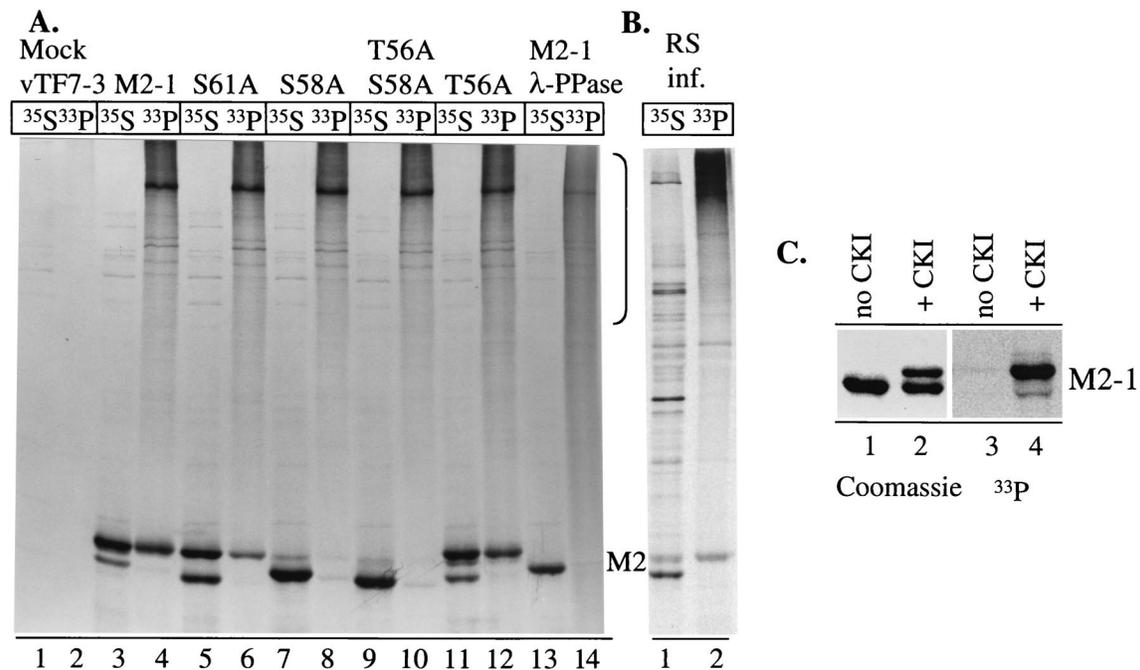
FIG. 2. Expression of M2-1 protein phosphorylation mutants. (A) Analysis of mutant proteins. HEp-2 cells, infected with vTF7-3, were either mock transfected or transfected with 5 μg of plasmids expressing M2-1 or the indicated phosphorylation mutants (S58A, S61A, T56A, or T56A S58A). The cells were labeled with either [^{35}S]methionine and [^{35}S]cysteine (^{35}S) or inorganic [^{33}P]phosphate (^{33}P) for 3 h at 17 h p.t. Cytoplasmic extracts were prepared and precleared. Then proteins were immunoprecipitated with MAb ICI3, separated by SDS-PAGE, and subjected to autoradiography. After immunoprecipitation, the samples in lanes 13 and 14 were treated with 200 U of λ-PPase for 30 min at 30°C. The bracket indicates the position of the ^{33}P-labeled coimmunoprecipitated material. (B) RS virus proteins. RS virus-infected (RS inf.) HEp-2 cells, harvested 24 h post infection, were prepared and immunoprecipitated as described for panel A, except the lysate was not precleared. (C) In vitro CKI phosphorylation of M2-1 protein. M2-1 protein produced in *E. coli* was incubated with CKI and [γ-^{33}P]ATP for 30 min at 37°C. The protein was separated by SDS-PAGE on an 11% polyacrylamide gel and Coomassie stained (left) or subjected to autoradiography (right).

context (14). The F/M2 replicon was chosen because of the sensitivity of the F/M2 gene junction to the action of the M2-1 protein (14). Previous work has shown that RS virus genes respond differently to the presence of M2-1 (14). Some genes, such as the SH gene, terminate efficiently in the absence or presence of M2-1, while others terminate inefficiently in the presence of M2-1. In the F/M2 replicon, there is a 15-fold increase in the percentage of full-length bicistronic readthrough products in the presence of M2-1 (14). The mRNA products transcribed by the F/M2 replicon have been described previously and are shown schematically in Fig. 3A (14). Transcription from this replicon results in the synthesis of two discrete mRNAs: mRNA1, produced from the upstream gene, and mRNA2, produced from the downstream gene. Three RNA products, resulting from the failure of the polymerase to terminate at the gene ends, thereby generating polycistronic or readthrough RNAs, are produced in increased amounts in the presence of M2-1. Readthrough (r/t) A is produced by the failure to terminate at the end of mRNA2. R/t B results from the failure to terminate at the F/M2 gene junction. R/t C is produced by the failure to terminate at both the F/M2 gene junction and the mRNA2 gene end. A stop codon was introduced into the M2 coding sequence in the F/M2 replicon to ensure that the replicon did not produce a truncated M2-1 protein, which could potentially obscure the effects of the phosphorylation mutants. MVA-infected HEp-2 cells were transfected with pN, pP, pL, pF/M2, and increasing amounts of

wt or mutant M2-1 plasmids. The effect of the M2-1 protein on transcriptional antitermination was measured by calculating the percentage of readthrough products, using molar amounts of the RNAs obtained from densitometry (14). The amounts of RNA corresponding to r/t B, r/t C, and mRNA1 that were determined by densitometric analysis were normalized to the uridine content of each. The percent readthrough that occurred was calculated by dividing the amount of RNAs that initiated at the first gene start but failed to terminate at the first gene end (r/t B and r/t C) by the total amount of RNA that initiated at the first gene start (mRNA1, r/t B, and r/t C). The following equation was used: percent readthrough = $100 \times$ (r/t B + r/t C)/(mRNA1 + r/t B + r/t C) (14). In the absence of M2-1, low levels of readthrough products, only about 6%, were observed (Fig. 3B, lane 1, and C). In the presence of wt M2-1, the levels of polycistronic readthrough RNA (r/t A, r/t B, and r/t C) increased significantly (Fig. 3B, lanes 2, 3, and 4). This occurred even at low levels of input plasmid (Fig. 3B, compare lanes 1 and 2, r/t B and r/t C). As reported previously, M2-1 protein rapidly reaches maximal transcriptional antitermination activity at input plasmid levels between 0.1 and 0.3 μg (16, 17). The S58A, S61A, and T56A S58A mutants all displayed reduced ability as antiterminators at low levels of input plasmid (Fig. 3B, lanes 5, 8, and 11, and C). At higher levels of input plasmid, they regained some activity, suggesting the mutants were less efficient but not completely impaired in activity (Fig. 3B, lanes 7, 10, and 13, and C). The activity of the S58A, S61A,
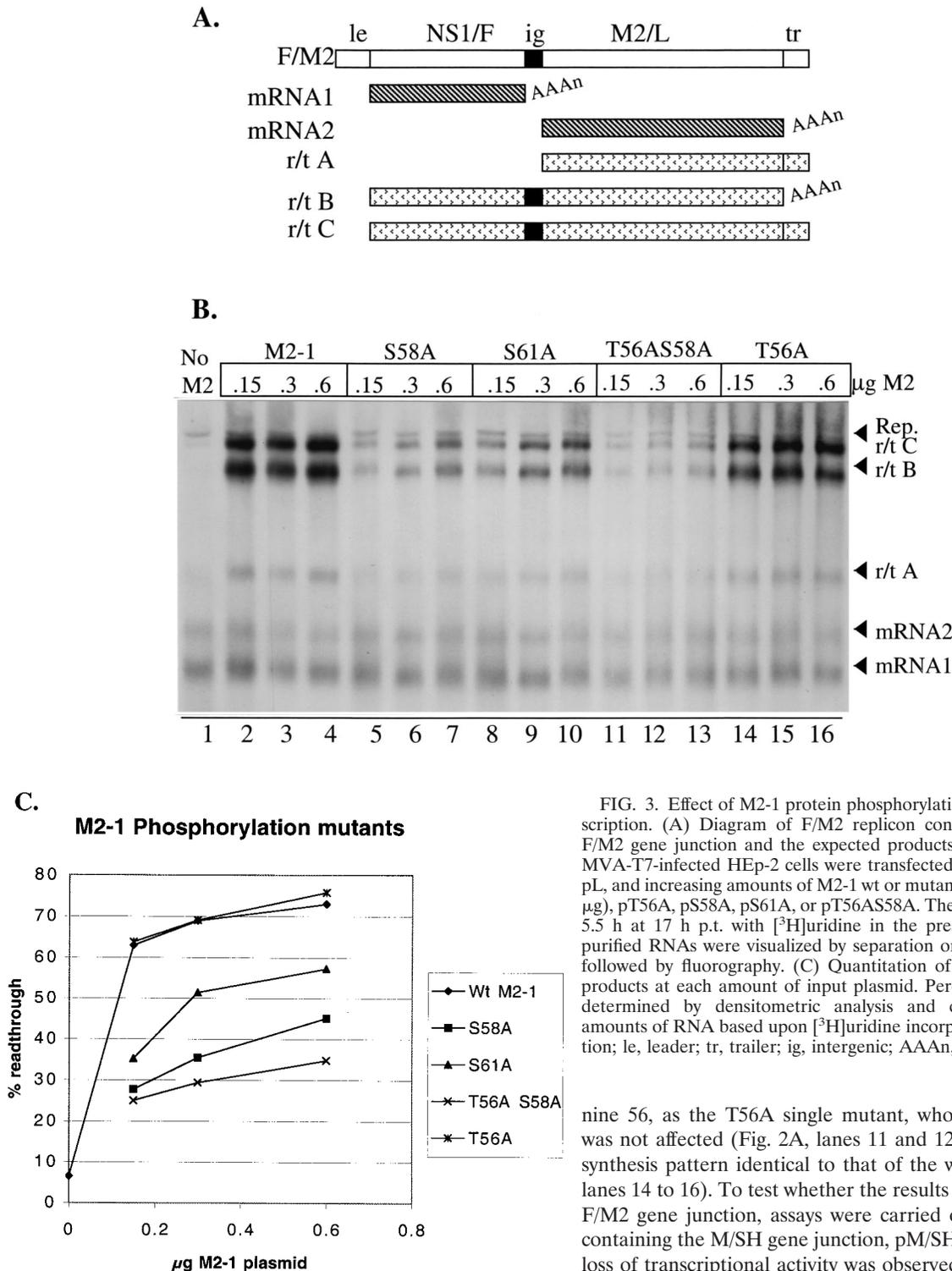
FIG. 3. Effect of M2-1 protein phosphorylation mutations on transcription. (A) Diagram of F/M2 replicon containing the authentic F/M2 gene junction and the expected products of transcription. (B) MVA-T7-infected HEp-2 cells were transfected with pF/M2, pN, pP, pL, and increasing amounts of M2-1 wt or mutant plasmids (0.15 to 0.6 µg), pT56A, pS58A, pS61A, or pT56AS58A. The cells were labeled for 5.5 h at 17 h p.t. with [³H]uridine in the presence of Act D. The purified RNAs were visualized by separation on an agarose-urea gel followed by fluorography. (C) Quantitation of percent readthrough products at each amount of input plasmid. Percent readthrough was determined by densitometric analysis and conversion to molar amounts of RNA based upon [³H]uridine incorporation. Rep, replication; le, leader; tr, trailer; ig, intergenic; AAAn, polyadenylate.

nine 56, as the T56A single mutant, whose phosphorylation was not affected (Fig. 2A, lanes 11 and 12), showed an RNA synthesis pattern identical to that of the wt protein (Fig. 3B, lanes 14 to 16). To test whether the results were specific to the F/M2 gene junction, assays were carried out with a replicon containing the M/SH gene junction, pM/SH (14), and a similar loss of transcriptional activity was observed (data not shown).

M2-1 interaction with RNA. As indicated in the discussion of Fig. 2A, a large amount of ³³P-labeled material, which migrated diffusely at the top of the gel, was coimmunoprecipitated with M2-1 protein or its phosphorylation mutants (Fig. 2A and Fig. 4A, lanes 2, 4, and 5). This represented a significant interaction, as it was not present in the immunoprecipitated mock-transfected lane (Fig. 4A, lane 1). To determine the nature of the coimmunoprecipitated component, the sam-
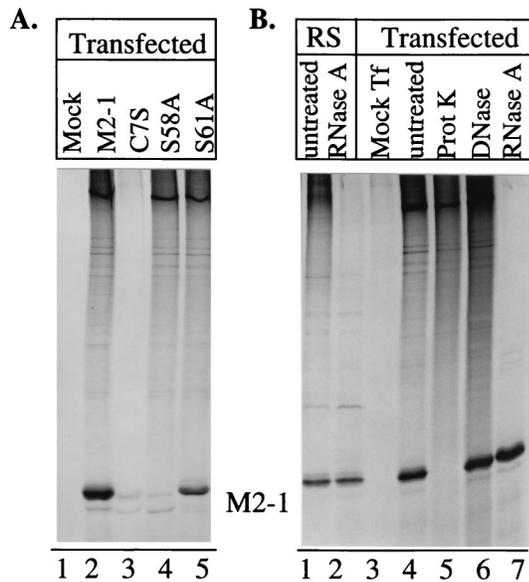
and T56A S58A mutants remained below that of the wt at all three input plasmid levels. The S61A mutant, which was not as impaired as the S58A and T56A S58A mutants, reached readthrough levels of about 55% (Fig. 3C). The T56A S58A double mutant was reproducibly the least efficient antiterminator. This inefficiency was not due to the mutation at threonine

FIG. 4. RNA is coimmunoprecipitated with the M2-1 protein. (A) HEp-2 cells infected with vTF7-3 were either mock transfected or transfected with 5 µg of pM2-ORF1 or plasmids expressing mutant M2-1 proteins. The cells were labeled for 3 h at 17 h p.t. with inorganic [³³P]phosphate. Immunoprecipitations were performed using MAb ICI3. The immunoprecipitated proteins were analyzed by SDS-PAGE on an 11% polyacrylamide gel followed by autoradiography. (B) Digestion of ³³P-labeled component. Transfected (lane 3, mock; lanes 4 to 7, 5 µg of pM2-ORF1) and infected (lanes 1 and 2) cells were prepared as for panel A, except 5 µg of proteinase K (Prot K), 5 µg of RNase A, or 1 U of DNase RQI was added after immunoprecipitation as indicated, followed by incubation for 30 min at 37°C.

ples were treated with DNase RQI, proteinase K, RNase A, or λ-PPase prior to PAGE. Digestion with λ-PPase, proteinase K, and DNase RQI did not affect the material coimmunoprecipitated by an M2-1-specific MAb (Fig. 2A, lane 14, and 4B, lanes 5 and 6). However, digestion with RNase A following immunoprecipitation resulted in the disappearance of this material (Fig. 4B, lane 7), suggesting the coimmunoprecipitated material was RNA. The ³³P-labeled material was also coimmunoprecipitated with M2-1 in the context of an RS virus infection, as well as in the transfections shown, where it was again susceptible to RNase A digestion (Fig. 4B, lanes 1 and 2). These results suggest that the M2-1 protein was interacting with RNA, which was coimmunoprecipitated with the M2-1 protein.

A previously characterized mutant, C7S, which contains a cysteine-to-serine change in one of the proposed zinc binding residues, was unable to coimmunoprecipitate RNA (Fig. 4A, lane 3). Previous work has shown that this mutant has lost its ability to function in transcription (15), indicating the need for maintenance of the zinc binding domain for function. It is also not efficiently phosphorylated, which we have attributed to improper folding due to disruption of the Cys3His1 motif, and as a result, very little ³³P-labeled protein was present in the ³³P-labeled sample (Fig. 4A, lane 3) (15). However, duplicate samples labeled with [³⁵S]methionine and [³⁵S]cysteine showed that levels of the C7S protein were similar to those in wt M2-1, providing evidence that the lack of an interaction with RNA was due to the disruption of the Cys3His1 motif and not to a lack of C7S protein (data not shown).

The above-mentioned coimmunoprecipitation experiments (Fig. 4) were performed under conditions where all the RNAs in the transfected or infected cells were labeled. We next examined the ability of the M2-1 protein to interact with RS virus RNAs in infected cells in the presence of Act D, which limits labeling to RNAs produced by the RS virus RdRp. HEp-2 cells were infected with RS virus, and RNAs were labeled with inorganic [³³P]phosphate. The cytoplasmic extracts were immunoprecipitated with MAbs to RS virus M2-1, N, or F protein, and the coimmunoprecipitated RNAs were extracted and analyzed by agarose-urea gel electrophoresis adjacent to total cytoplasmic RNA from an RS virus infection. The anti-M2-1 MAb, ICI3, predominately coimmunoprecipitated RNAs that comigrated with RS virus monocistronic and polycistronic mRNAs (Fig. 5, compare lanes 2 and 3). Upon longer exposure of the film, a genomic band was also detected (data not shown). As controls, MAbs to RS virus N protein or F protein, MAb 15 and MAb 19, respectively, were used to immunopre-
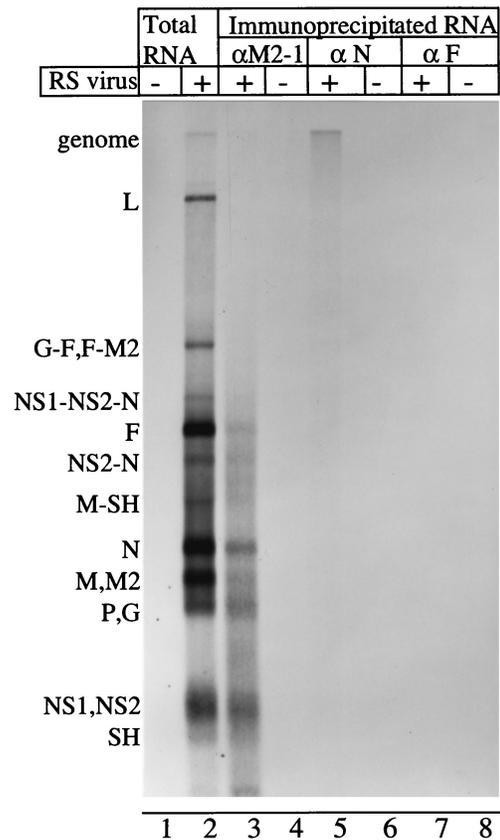

FIG. 5. Analysis of coimmunoprecipitated RNA from an RSV infection. HEp-2 cells in 100-mm-diameter dishes were infected with RS virus (MOI = 10). The cells were labeled in the presence of Act D at 17 h postinfection for 5 h with inorganic [³³P]phosphate. Cytoplasmic extracts were prepared, and lysates were either immunoprecipitated with MAbs to the M2-1, N, or F protein or analyzed for total RNA. RNAs were released from the immunoprecipitation mixture by boiling it in NTE. Immunoprecipitated and total RS virus RNAs were purified by phenol extraction and ethanol precipitation, followed by separation on an agarose-urea gel and fluorography. The locations of the various RS virus monocistronic and polycistronic RNAs are indicated on the left. +, present; −, absent.
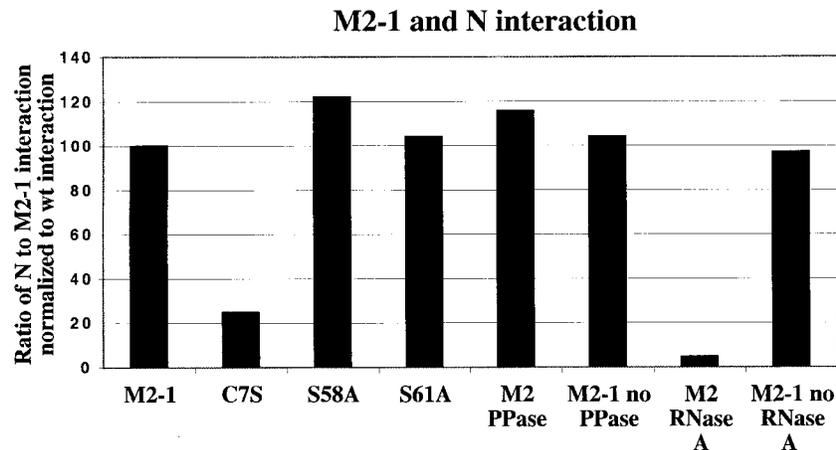
M2-1 and N interaction

FIG. 6. M2-1 protein–N protein interaction is unaffected by phosphorylation but is sensitive to RNase A digestion. HEp-2 cells infected with vTF7-3 were transfected with 5 μg of the indicated plasmid(s). The cells were labeled 17 h p.t. for 3 h with [^{35}S]methionine and [^{35}S]cysteine and immunoprecipitated with ICI3. RNase A (5 μg) and λ-PPase (200 U) were added as indicated, and samples were incubated at 37 or 30°C, respectively, for 30 min. Control samples for the RNase A and λPPase reactions were treated identically to the digested samples, except that the RNase A and λPPase were omitted. The treated and control samples were washed to remove any released protein and analyzed by electrophoresis on an 11% polyacrylamide gel. The percent M2-1–N interaction normalized to the wt interaction was quantified by densitometric analysis of autoradiograms for each sample.

cipitate duplicate samples. RS virus genomic RNA was primarily coimmunoprecipitated by the anti-N MAb, as expected, since the genome is encapsidated with N protein (Fig. 5, lane 5) (36). The anti-F MAb did not immunoprecipitate any detectable RNA (Fig. 5, lane 7). In addition, immunoprecipitation of lysate from uninfected cells showed no detectable RNAs (Fig. 5, lanes 4, 6, and 8). In similar experiments where Act D was omitted so both cellular and viral RNAs were labeled, RS viral RNAs were still coimmunoprecipitated, although it was clear that cellular RNAs, in particular rRNAs, were also coimmunoprecipitated (data not shown). These results indicated that during RS virus infection, M2-1 protein can associate with RS virus mRNA in an interaction strong enough to withstand the multiple manipulations and washings associated with the immunoprecipitation procedure. It could be argued that M2-1 interacts with RNA through interaction with another viral protein; however, the coimmunoprecipitation experiment from transfected cells (Fig. 4) and a recently published report (9) both showed that M2-1 interacted with RNA in the absence of the other viral proteins. However, it is possible that other viral proteins play a role in determining the specificity of the interaction of M2-1 with RNA.

M2-1 interaction with N protein. Previous work has shown that M2-1 interacts with the N protein in cotransfected cells (12, 15). To assay whether phosphorylation was necessary for the interaction, the phosphorylation mutants were tested for the ability to interact with the N protein. Plasmids expressing the M2-1 protein or the M2-1 phosphorylation mutants and N protein were cotransfected into HEp-2 cells, which were labeled with [^{35}S]methionine and [^{35}S]cysteine. The lysates were immunoprecipitated with the anti-M2-1 MAb, ICI3. In the presence of wt M2-1 protein, a significant amount of N protein was coimmunoprecipitated (Fig. 6). The previously characterized C7S mutant is unable to interact with N and thus coimmunoprecipitated very little N protein, as expected (Fig. 6). The two phosphorylation mutants, S58A and S61A, coimmu-

noprecipitated levels of N similar to that coimmunoprecipitated by wt M2-1 (Fig. 6). In addition, treatment of the immunoprecipitated material with λ-PPase did not affect the ability of M2-1 to coimmunoprecipitate N (Fig. 6). These results suggest that phosphorylation of the M2-1 protein was not necessary for interaction with the N protein. It was suggested previously that the M2-1–N interaction may be mediated via another component because of a lack of interaction when the proteins were synthesized in vitro using rabbit reticulocyte lysate (12). Since the results of the previous experiments indicated that M2-1 interacts with RNA, we tested whether RNA could mediate the M2-1–N interaction. Treatment of the M2-1–N protein interaction with RNase A followed by washing reduced the amount of coimmunoprecipitated N to background levels (5% of the wt interaction) (Fig. 6). These data indicated that the interaction between M2-1 and N in cotransfected cells was mediated via RNA. Thus, the experiments assessing the ability of the M2-1 phosphorylation mutants to interact with the N protein may instead be an indirect reflection of their ability to interact with RNA.

DISCUSSION

We examined the sites of phosphorylation and the role that phosphorylation plays in the function of the M2-1 protein in transcription and interaction with viral RNA. The M2-1 protein was found by proteolytic digestion and site-directed mutagenesis to be phosphorylated at serine 58 and serine 61. Serines 58 and 61 lie in the consensus sequence for phosphorylation by CKI and are conserved in human, bovine, and ovine RS virus and in turkey rhinotracheitis virus (1, 8, 26, 29, 35, 37). The conservation of these residues suggests a functional role for M2-1 phosphorylation. Phosphorylation of serine 58 creates a new CKI site at serine 61. The disruption of serine 58 should prevent phosphorylation at serine 61, which would result in the loss of both phosphorylation sites, which is consis-

tent with our results. Based on sequence analysis, mutation at serine 61 would be expected to affect phosphorylation at only that site and not at serine 58, explaining why the S61A mutant retains ^{33}P incorporation. The above observations are consistent with our results. In addition, bacterially expressed M2-1 protein was shown to be phosphorylated twice by CKI on a fragment corresponding to amino acids 53 to 92, which contains the phosphorylation sites determined by site-directed mutagenesis, serine 58 and serine 61. A recent report concluded that threonine 56 and serine 58 were the main phosphorylation sites in M2-1 (9). These workers analyzed M2-1 phosphorylation in the context of a double mutant in which threonine 56 and serine 58 were both changed to alanine (9). The protein also contained an internal deletion between amino acids 110 and 166. This mutant lost 98% of its phosphorylation compared to the parent protein. The result observed from the double mutant can be attributed solely to the mutation at serine 58, because of its ability to affect the potential phosphorylation of serine 61. As shown in the results of this paper, the T56A single mutant is unaltered in its phosphorylation state compared to the wt protein, and this mutation has no effect on M2-1 function. Therefore, threonine 56 does not substantially contribute to the phosphorylation of M2-1 or to its function. Our results show that serines 58 and 61 are the major phosphorylation sites. It should be noted that M2-1 may contain an additional minor phosphorylation site, as the S58A and T56A S58A mutants both show very low levels of ^{33}P incorporation.

Mutation of the phosphorylated residues, serines 58 and 61, to alanine resulted in a decrease in the efficiency of M2-1 protein transcriptional antitermination activity, as assayed by the effect on transcription of a subgenomic replicon containing the F/M2 gene junction. Increasing the level of input mutant M2-1-encoding plasmids allowed a low level of increase in transcriptional antitermination activity, but never to a level equivalent to that seen with wt M2-1 protein, suggesting the mutant proteins are inefficient antiterminators. The defect in antitermination does not appear to be due to an inability to bind RNA, as the phosphorylation mutants coimmunoprecipitated RNA as well as the wt protein. Rather, the defect may be in RNA binding specificity or in the ability to function once bound to RNA. It is interesting that during an RS virus infection, the unphosphorylated form of M2-1 is the predominant form of the protein. This differs from conditions under which M2-1 is transfected by itself, where the phosphorylated form is predominant, an observation that may suggest that control over the extent of M2-1 phosphorylation exists during infection. Previous analyses have indicated that the presence of other RS virus proteins, such as the P protein, affect the level of M2-1 phosphorylation (Hardy, unpublished) (9). There are numerous examples of prokaryotic and eukaryotic transcription factors that use phosphorylation as a means to positively or negatively control activity (18, 31). In addition, the M2-1 protein is not the only RS virus protein whose function is tied to phosphorylation, as phosphorylation of the RS virus P protein increases its efficiency in transcription and replication (27, 33). However, it remains to be determined whether M2-1 function during RS virus infection is regulated by phosphorylation or whether the different phosphoforms of M2-1 have additional functions as yet undetermined. In addition, further work

is necessary and is under way to determine if the processivity activity of M2-1 is also affected by phosphorylation.

The ability of M2-1 to coimmunoprecipitate RNA from transfected cells led to the discoveries that during infection M2-1 can associate with RS virus mRNAs and that the previously observed interaction between the M2-1 and N proteins in cotransfected cells was mediated via RNA. The results from the M2-1–N interaction experiment indicated that the M2-1 and N proteins were interacting by binding to the same RNA (Fig. 6), yet immunoprecipitation from RS virus-infected cells with the N MAb showed that the N protein interacted with genomic RNA, as expected for the nucleocapsid protein (Fig. 5, lane 5), while the M2-1 MAb predominately coimmunoprecipitated mRNA (Fig. 5, lane 3). The analysis of the M2-1–N interaction (Fig. 6) was performed in transfected cells and not in the context of an RS virus infection, and it is likely that the M2-1 and N proteins, like many other RNA binding proteins, were binding RNAs promiscuously in the absence of their natural substrates, possibly by binding the mRNAs produced from the M2-1- and N-encoding plasmids, as they were the only RS virus RNAs present in the cells.

In separate work, Cuesta et al. also recently reported that M2-1 is an RNA binding protein (9). They concluded that the M2-1 protein bound specifically to the antigenomic leader sequence of the RS virus RNA and nonspecifically to "long" RNAs. Our results show that during RS virus infection, M2-1 interacts predominately with viral mRNAs, which do not contain the leader sequence. Clearly, further work is necessary to analyze the specificity of RNA binding by M2-1 and to determine whether other viral proteins are involved in determining the specificity of M2-1 interaction with RNA.

The observation that the M2-1 protein interacts with RNA is consistent with the fact that many proteins that function in transcription and contain zinc binding motifs also bind nucleic acids. M2-1 protein contains a Cys3His1 zinc binding motif at its amino terminus. The best-described member of the Cys3His1 class of zinc fingers is tristetraprolin (TTP), an RNA binding protein whose function, like that of M2-1, is dependent upon the integrity of its Cys3His1 motif. Mutation of a single zinc-coordinating residue in TTP results in a loss of RNA binding (22). It is interesting that the C7S mutant, which is defective in antitermination (15), is also defective in RNA binding, as assayed by immunoprecipitation (Fig. 4A, lane 3).

In conclusion, we have demonstrated that M2-1 is phosphorylated at serines 58 and 61. Phosphorylation is required for the efficient transcriptional function of M2-1, as mutation of serines 58 and 61 results in a severe decrease of antitermination activity. We have also shown that M2-1 is associated with viral monocistronic and polycistronic mRNA during RS virus infection. Maintenance of the Cys3His1 motif, but not phosphorylation, is required for interaction with RNA. In addition, the interaction between the M2-1 and N proteins is mediated via RNA.

REFERENCES

1. **Alansari, H., and L. N. Potgieter.** 1994. Molecular cloning and sequence analysis of the phosphoprotein, nucleocapsid protein, matrix protein and 22K (M2) protein of the ovine respiratory syncytial virus. J. Gen. Virol. **75:**3597–3601.
2. **Barik, S.** 1992. Transcription of human respiratory syncytial virus genome RNA in vitro: requirement of cellular factor(s). J. Virol. **66:**6813–6818.
3. **Collins, P. L., L. E. Dickens, A. Buckler-White, R. A. Olmsted, M. K. Spriggs, E. Camargo, and K. V. Coelingh.** 1986. Nucleotide sequences for the gene junctions of human respiratory syncytial virus reveal distinctive features of intergenic structure and gene order. Proc. Natl. Acad. Sci. USA **83:**4594–4598.
4. **Collins, P. L., M. G. Hill, J. Cristina, and H. Grosfeld.** 1996. Transcription elongation factor of respiratory syncytial virus, a nonsegmented negative-strand RNA virus. Proc. Natl. Acad. Sci. USA **93:**81–85.
5. **Collins, P. L., M. G. Hill, and P. R. Johnson.** 1990. The two open reading frames of the 22K mRNA of human respiratory syncytial virus: sequence comparison of antigenic subgroups A and B and expression in vitro. J. Gen. Virol. **71:**3015–3020.
6. **Collins, P. L., Y. T. Huang, and G. W. Wertz.** 1984. Identification of a tenth mRNA of respiratory syncytial virus and assignment of polypeptides to the 10 viral genes. J. Virol. **49:**572–578.
7. **Collins, P. L., and G. W. Wertz.** 1983. cDNA cloning and transcriptional mapping of nine polyadenylylated RNAs encoded by the genome of human respiratory syncytial virus. Proc. Natl. Acad. Sci. USA **80:**3208–3212.
8. **Collins, P. L., and G. W. Wertz.** 1985. The envelope-associated 22K protein of human respiratory syncytial virus: nucleotide sequence of the mRNA and a related polytranscript. J. Virol. **54:**65–71.
9. **Cuesta, I., X. Geng, A. Asenjo, and N. Villanueva.** 2000. Structural phosphoprotein M2-1 of the human respiratory syncytial virus is an RNA binding protein. J. Virol. **74:**9858–9867.
10. **Dickens, L. E., P. L. Collins, and G. W. Wertz.** 1984. Transcriptional mapping of human respiratory syncytial virus. J. Virol. **52:**364–369.
11. **Fearns, R., and P. L. Collins.** 1999. Role of the M2-1 transcription antitermination protein of respiratory syncytial virus in sequential transcription. J. Virol. **73:**5852–5864.
12. **Garcia, J., B. Garcia-Barreno, A. Vivo, and J. A. Melero.** 1993. Cytoplasmic inclusions of respiratory syncytial virus-infected cells: formation of inclusion bodies in transfected cells that coexpress the nucleoprotein, the phosphoprotein, and the 22K protein. Virology **195:**243–247.
13. **Grosfeld, H., M. G. Hill, and P. L. Collins.** 1995. RNA replication by respiratory syncytial virus (RSV) is directed by the N, P, and L proteins; transcription also occurs under these conditions but requires RSV superinfection for efficient synthesis of full-length mRNA. J. Virol. **69:**5677–5686.
14. **Hardy, R. W., S. B. Harmon, and G. W. Wertz.** 1999. Diverse gene junctions of respiratory syncytial virus modulate the efficiency of transcription termination and respond differently to M2-mediated antitermination. J. Virol. **73:**170–176.
15. **Hardy, R. W., and G. W. Wertz.** 2000. The Cys(3)-His(1) motif of the respiratory syncytial virus M2-1 protein is essential for protein function. J. Virol. **74:**5880–5885.
16. **Hardy, R. W., and G. W. Wertz.** 1998. The product of the respiratory syncytial virus M2 gene ORF1 enhances readthrough of intergenic junctions during viral transcription. J. Virol. **72:**520–526.
17. **Harmon, S. B., A. G. Megaw, and G. W. Wertz.** 2001. RNA sequences involved in transcriptional termination of respiratory syncytial virus. J. Virol. **75:**36–44.
18. **Hunter, T., and M. Karin.** 1992. The regulation of transcription by phosphorylation. Cell **70:**375–387.
19. **Jacques, J. P., and D. Kolakofsky.** 1991. Pseudo-templated transcription in prokaryotic and eukaryotic organisms. Genes Dev. **5:**707–713.
20. **Kuo, L., R. Fearns, and P. L. Collins.** 1997. Analysis of the gene start and gene end signals of human respiratory syncytial virus: quasi-templated initiation at position 1 of the encoded mRNA. J. Virol. **71:**4944–4953.
21. **Kuo, L., H. Grosfeld, J. Cristina, M. G. Hill, and P. L. Collins.** 1996. Effects of mutations in the gene-start and gene-end sequence motifs on transcription of monocistronic and dicistronic minigenomes of respiratory syncytial virus. J. Virol. **70:**6892–6901.
22. **Lai, W. S., E. Carballo, J. R. Strum, E. A. Kennington, R. S. Phillips, and P. J. Blackshear.** 1999. Evidence that tristetraprolin binds to AU-rich elements and promotes the deadenylation and destabilization of tumor necrosis factor alpha mRNA. Mol. Cell. Biol. **19:**4311–4323.
23. **Lambert, D. M., J. Hambor, M. Diebold, and B. Galinski.** 1988. Kinetics of synthesis and phosphorylation of respiratory syncytial virus polypeptides. J. Gen. Virol. **69:**313–323.
24. **Laskey, R. A.** 1980. The use of intensifying screens or organic scintillators for visualizing radioactive molecules resolved by gel electrophoresis. Methods Enzymol. **65:**363–371.
25. **Liao, P. C., J. Leykam, P. C. Andrews, D. A. Gage, and J. Allison.** 1994. An approach to locate phosphorylation sites in a phosphoprotein: mass mapping by combining specific enzymatic degradation with matrix-assisted laser desorption/ionization mass spectrometry. Anal. Biochem. **219:**9–20.
26. **Ling, R., A. J. Easton, and C. R. Pringle.** 1992. Sequence analysis of the 22K, SH and G genes of turkey rhinotracheitis virus and their intergenic regions reveals a gene order different from that of other pneumoviruses. J. Gen. Virol. **73:**1709–1715.
27. **Mazumder, B., and S. Barik.** 1994. Requirement of casein kinase II-mediated phosphorylation for the transcriptional activity of human respiratory syncytial viral phosphoprotein P: transdominant negative phenotype of phosphorylation-defective P mutants. Virology **205:**104–111.
28. **Pattnaik, A. K., and G. W. Wertz.** 1990. Replication and amplification of defective interfering particle RNAs of vesicular stomatitis virus in cells expressing viral proteins from vectors containing cloned cDNAs. J. Virol. **64:**2948–2957.
29. **Pinna, L. A., and M. Ruzzene.** 1996. How do protein kinases recognize their substrates? Biochim. Biophys. Acta **1314:**191–225.
30. **Routledge, E. G., M. M. Willcocks, L. Morgan, A. C. Samson, R. Scott, and G. L. Toms.** 1987. Heterogeneity of the respiratory syncytial virus 22K protein revealed by Western blotting with monoclonal antibodies. J. Gen. Virol. **68:**1209–1215. (Erratum, **68:**2272.)
31. **Rutberg, B.** 1997. Antitermination of transcription of catabolic operons. Mol. Microbiol. **23:**413–421.
32. **Stec, D. S., M. G. Hill, and P. L. Collins.** 1991. Sequence analysis of the polymerase L gene of human respiratory syncytial virus and predicted phylogeny of nonsegmented negative-strand viruses. Virology **183:**273–287.
33. **Villanueva, N., R. Hardy, A. Asenjo, Q. Yu, and G. Wertz.** 2000. The bulk of the phosphorylation of human respiratory syncytial virus phosphoprotein is not essential but modulates viral RNA transcription and replication. J. Gen. Virol. **81:**129–133.
34. **Wertz, G. W., and N. Davis.** 1981. Characterization and mapping of RNase III cleavage sites in VSV genome RNA. Nucleic Acids Res. **9:**6487–6503.
35. **Yu, Q., P. J. Davis, T. D. Brown, and D. Cavanagh.** 1992. Sequence and in vitro expression of the M2 gene of turkey rhinotracheitis pneumovirus. J. Gen. Virol. **73:**1355–1363.
36. **Yu, Q., R. W. Hardy, and G. W. Wertz.** 1995. Functional cDNA clones of the human respiratory syncytial (RS) virus N, P, and L proteins support replication of RS virus genomic RNA analogs and define minimal *trans*-acting requirements for RNA replication. J. Virol. **69:**2412–2419.
37. **Zamora, M., and S. K. Samal.** 1992. Sequence analysis of M2 mRNA of bovine respiratory syncytial virus obtained from an F-M2 dicistronic mRNA suggests structural homology with that of human respiratory syncytial virus. J. Gen. Virol. **73:**737–741.